We are IntechOpen, the world's leading publisher of Open Access books Built by scientists, for scientists

4,800
Open access books available

122,000
International authors and editors

135M
Downloads

Our authors are among the

154
Countries delivered to

TOP 1%
most cited scientists

12.2%
Contributors from top 500 universities

CLARIVATE ANALYTICS BOOK CITATION INDEX INDEXED

WEB OF SCIENCE™

Selection of our books indexed in the Book Citation Index in Web of Science™ Core Collection (BKCI)

Interested in publishing with us?
Contact book.department@intechopen.com

Numbers displayed above are based on latest data collected.
For more information visit www.intechopen.com

22

High-Carbon Alcohol Aqueous Solutions and Their Application to Flow Boiling in Various Mini-Tube Systems

Naoki Ono, Atsushi Hamaoka, Yuki Eda and Koichi Obara
Department of Engineering Science and Mechanics,
Shibaura Institute of Technology,
Japan

1. Introduction

The temperature dependence of the surface tension of certain high-carbon alcohol aqueous solutions such as those of butanol and pentanol is nonlinear. That is, the surface tension of the solution increases when it is heated beyond a certain temperature. Since this was discovered by Vochten et al. (Vochten & Petre, 1973) about 30 years ago, several experimental studies have examined the liquid motion of these alcohol aqueous solutions, focusing on how they differ from normal fluids. Simultaneously, several studies have attempted to apply the phenomenon to heat pipes (Abe, 2006a, 2006b) and other equipment to enhance heat transfer. The direction of the thermocapillary force in a liquid film of a nonlinear solution on a heated surface acts in the same direction as the solutocapillary force. This characteristic is expected to be remarkable in small-scale systems such as mini or micro channels.

In this chapter, the authors report the following three findings: 1) new measurement results regarding the nonlinear temperature dependence of the surface tension of high-carbon alcohol aqueous solutions, 2) a simple application of the solution to flow boiling in a straight mini tube and 3) modified applications of the solution to flow boiling in a T-junction mini tube.

Future applications of this study include miniature cooling systems such as those for CPUs and laser emitting devices although the use of a high-carbon alcohol aqueous solution would require further improvements and greater sophistication to be viable. Also, the precise mechanism of the combined force of the thermocapillary and solutocapillary effects need to be further investigated.

2. Temperature dependence of the surface tension of high-carbon alcohol aqueous solutions

The surface tension of normal fluids decreases as their temperature increases. However, as aforementioned, in alcohol aqueous solutions such as those of butanol and pentanol, surface tension increases as the temperature rises above a certain point. The behaviour of fluids with this special characteristic (called 'nonlinear thermocapillarity' here) has been investigated by numerous researchers (Legros, 1986; Azouni & Petre, 1998)

However, the temperature dependence of nonlinear thermocapillary solutions has not been completely measured, and it is little publicized except for Vochten's paper (Vochten & Petre, 1973). A reason for this is that it is somewhat difficult to technically reproduce Vochten's data because the procedure requires careful handling and heating of the solution. Moreover, in their study, concentration dependence was not investigated. A detailed investigation of concentration dependence is one of the aims of the present study.

The authors first adopted Wilhelmy's method and measured the surface tension of the solution during heating. However, this method requires a hole in the container's lid for hanging a wire. Therefore, the vapour of the test fluid can escape from the container, and thus, decreasing its concentration and affecting the measured value when the test fluid is an alcohol aqueous solution. After detecting this problem, the authors decided to adopt the maximum bubble pressure method instead.

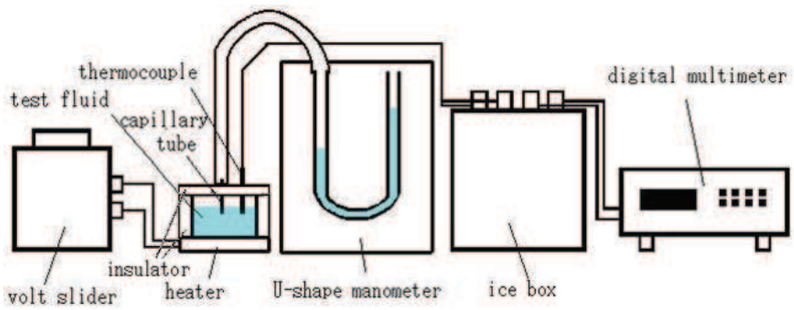

Fig. 1. Experimental apparatus for the maximum bubble pressure method.

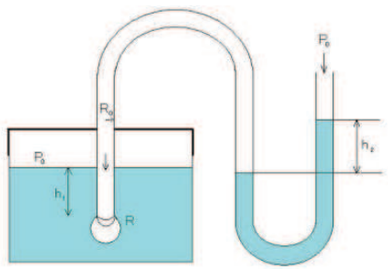

Fig. 2. Balance of static pressure in the maximum bubble pressure method.

Figure 1 shows a schematic of the measurement setup of the maximum bubble pressure method. The basic principle of this technique can be found in numerous reference books (e.g. Adamson & Gast, 1997). A fine capillary tube is immersed in a test fluid and air is pushed into the tube from its rear end. Thus, small semi-spherical bubbles are generated at the tube end immersed in the test fluid. This method detects the internal pressure at the instant when the bubble detaches from the capillary tube. The authors attached a U-shaped manometer tube, which enables increasing the internal pressure and measuring the head length (Ono et al., 2008b, 2009).

Figure 2 shows the pressure balance among the atmospheric pressure, the fluid static pressure, and the head difference in the manometer. When the tube end is located at h_1, i.e. below the fluid free surface, and the radius of curvature of the bubble is R, the pressure inside the bubble $p(R)$ can be expressed in two ways. One uses the fact that $p(R)$ is equal to the pressure inside the manometer. The other uses the fact that $p(R)$ is equal to the static pressure in the fluid container. Thus, the following equation can be obtained.

$$p(R) = p_0 + \rho g h_1 + \frac{2\gamma}{R} = p_0 + \rho g h_2 \tag{1}$$

The expression for surface tension can then be deduced as follows.

$$\gamma = \frac{\rho g (h_2 - h_1) R}{2} \tag{2}$$

Whenever static balance is achieved, Eq. (2) is satisfied. Because a pressure increment is applied inside the manometer, the radius R of the bubble decreases; its minimum value is achieved when the bubble radius becomes equal to the tube's inner radius R_0. Then, the bubble radius again increases; however, in most cases, the bubble detaches from the tube as soon as the radius increases. When the bubble radius is minimum, the Laplace pressure becomes maximum. Thus, surface tension can be deduced from Eq. (2) by using the pressure balance at this instant and by setting R to R_0.

A glass tube that was 32 mm long with an inner diameter (ID) of 0.20 mm and outer diameter (OD) of 0.68 mm, was used as the capillary tube. The tube was specially prepared with high precision. The precision of the diameter was 0.01 mm. The tube was connected to a U-shaped manometer, which measures the internal pressure. By adding a small drop of pure water into the manometer, the internal pressure was increased; air was gradually forced into the test liquid. At the instant when a bubble detaches from the capillary tube, the maximum pressure can be measured using the head difference in the U-shaped manometer because the bubble radius becomes approximately equal to the tube inner radius at bubble detachment.

Pure water was used as the fluid inside the manometer for simplicity and the ease of handling and because alcohol aqueous solutions in low concentration used here have approximately the same density as pure water. The test fluid was held in a glass container with an inner diameter of 60 mm and the bottom of the container was heated. The glass container was covered with a holder and a lid made of an insulating material. A capillary tube and thermocouple were attached to the lid and inserted into the test fluid. The lid keeps the vapour from escaping the container. In these experiments, to maintain atmospheric pressure, the lid was equipped with a small vinyl balloon to absorb the volume expansion of the gas phase inside the container. The fluid temperature was slowly increased from room temperature at increments of 5 °C. After confirming that the temperature was constant and steady, the temperature was measured.

The test fluids used in this study were 1-butanol aqueous solution, 1-pentanol aqueous solution, ethanol aqueous solution and pure water. Moreover, pure 1-butanol and 1-pentanol were analysed for comparison. Henceforth, 1-butanol and 1-pentanol are referred to simply as butanol and pentanol.

Wilhelmy's method was employed to obtain data for comparison with those obtained by the maximum bubble pressure method. The measuring technique in this study was explained by the authors' group in an earlier work (Ono et al., 2009). A schematic of the apparatus for Wilhelmy's method is shown in Fig. 3. In this study, the force caused by surface tension was measured at the instant when the platinum plate was detached from the liquid. This method requires a hole. Therefore, the influence of evaporation of the solution cannot be eliminated in this method.

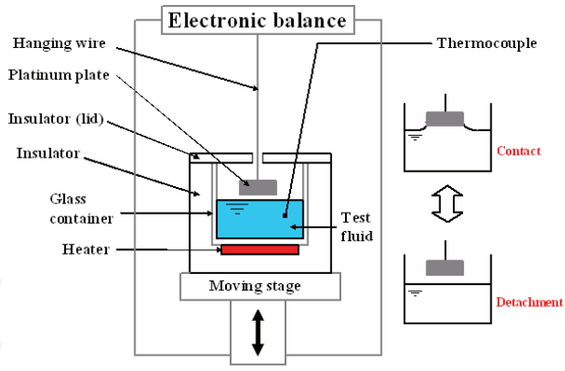

Fig. 3. Experimental apparatus for Wilhelmy's method.

Figure 4 compares the data for pure water obtained by Wilhelmy's method with those obtained by the maximum bubble pressure method. In the figure, 'wilhelmy' indicates data obtained by Wilhelmy's method and 'bubble' indicates those obtained by the maximum bubble pressure method. This notation is also used in all of the following figures. The evaporation of pure water has no effect on measured values even in Wilhelmy's method because the concentration does not matter. According to Fig. 4, data measured by the static maximum bubble pressure method agreed well with those obtained by Wilhelmy's method. Moreover, the data obtained by the maximum bubble pressure method were compared with published JSME data (Japanese Society of Mechanical Engineers, 1983) as follows. At 30 °C, σ = 70.6 (mN/m) (bubble method) and 71.19 (mN/m) (JSME data). (All subsequent values are presented in this order.) At 50 °C, σ = 67.6 and 67.94. At 70 °C, σ = 64.3 and 64.47. At 90 °C, σ = 60.7 and 60.8. Thus, the deviation from the JSME data was 0.1–0.4 mN/m, which is reasonably small. The above two comparisons confirm that the maximum bubble pressure method has sufficient validity.

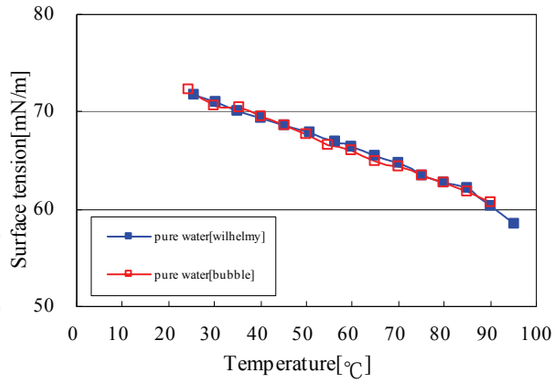

Fig. 4. Pure water data obtained using the maximum bubble pressure method and Wilhelmy's method.

Figure 5 shows measured data for aqueous solutions of butanol, pentanol and ethanol each of which have representative alcohol concentrations. The figure compares the data obtained by the maximum bubble pressure method with those obtained by Wilhelmy's method. The peculiar behaviour of interest, namely, the tendency for surface tension to increase at temperatures above a critical temperature, is seen for butanol and pentanol aqueous solutions. The data obtained by the maximum bubble pressure method show a smaller

increase with increasing temperature. This is attributed to the elimination of the escaping vapour in the maximum bubble pressure method. The effect of the escaping vapour on the alcohol concentration in Wilhelmy's method, which was employed in the previous study (Ono et al., 2009), was not negligible, and the maximum bubble pressure method used in this study successfully prevented this problem. The authors believe that more reliable data were obtained in this study.

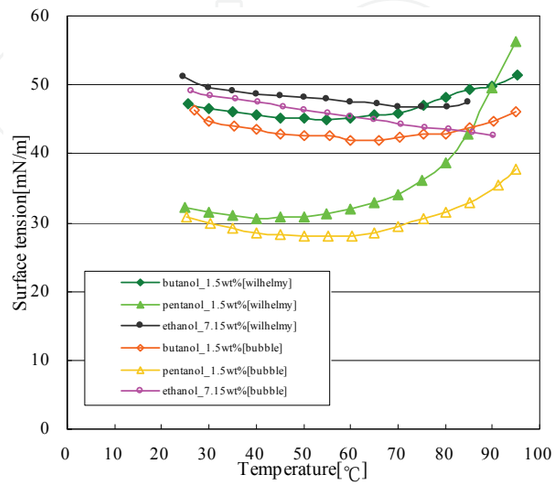

Fig. 5. Comparison of the maximum bubble pressure method and Wilhelmy's method for various solutions.

Figure 6 shows measured results for butanol aqueous solutions. As the temperature increased, the surface tension of most butanol solutions decreased up to approximately 60 °C. Above 60 °C, the surface tension started to increase. At higher concentrations, the absolute value of surface tension was lower, and the nonlinearity was greater. Figure 6 includes results for pure butanol, which is referred to as butanol. As expected, the surface tension of butanol decreased monotonically, as it was heated. This tendency differs significantly from that of alcohol aqueous solutions.

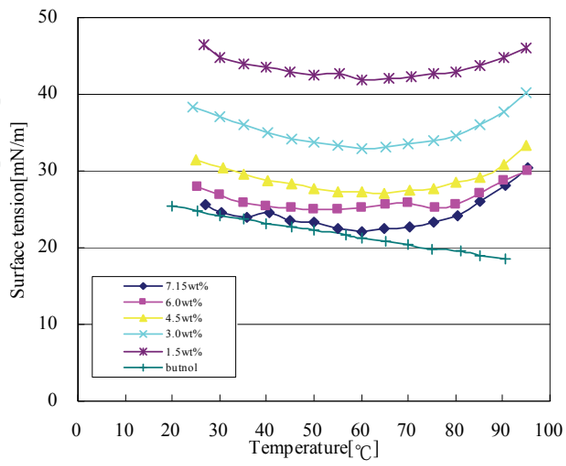

Fig. 6. Surface tension of butanol aqueous solutions measured by the maximum bubble pressure method.

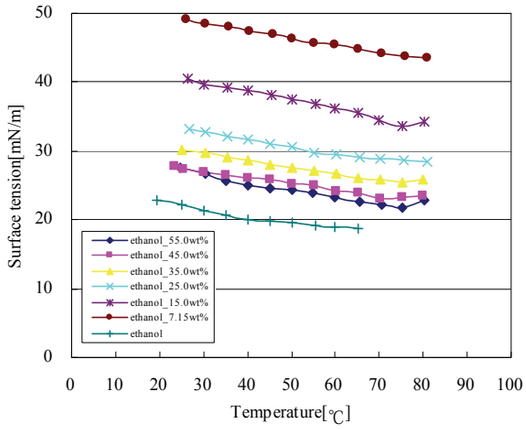

Fig. 7. Surface tension of ethanol aqueous solutions measured by the maximum bubble pressure method.

Figure 7 shows results for ethanol aqueous solutions. All lines tend to decrease monotonically as the temperature increases. However, surface tension remained constant and increased slightly at temperatures above 75 °C. The authors believe that this could be the result of instability caused by boiling because the boiling point of these solutions is approximately 80 °C.

The maximum bubble pressure method found a milder nonlinearity for the surface tension of butanol and pentanol aqueous solutions than Wilhelmy's method, as shown in Fig. 5. The authors believe that because the maximum bubble pressure method encloses the test fluid and the vapour, the error caused by changes in concentration because of species evaporation was greatly minimized. This condition is very different from that employed in Wilhelmy's method. The authors consider the maximum bubble pressure method and procedure used in this study gave more reasonable and reliable values.

The solubility of butanol in pure water at room temperature is 7.15 wt% and that of pentanol in pure water at room temperature is 2.0 wt%. The surface tension of pure water is very sensitive to the addition of these alcohols. At solubility concentrations, the surface tension of alcohol aqueous solutions approached that of pure alcohols at low temperature, as shown in Fig. 6.

On the other hand, the ethanol aqueous solutions varied in their temperature dependence, as shown in Fig. 7. The solubility concentration is not 55 wt%. If the concentration of ethanol was increased further, the line would approach that of pure ethanol.

In summary, by performing these measurements, the authors themselves re-confirmed the peculiar dependence of surface tension on temperature in high-carbon alcohol aqueous solutions. The nonlinearity of the behaviour was milder than that expected from measurements using the traditional Wilhelmy's method. The maximum bubble pressure method yielded very reasonable data. The authors then began flow boiling experiments with those peculiar solutions and attempted to determine their advantages in terms of heat transfer enhancement.

3. Simple application to flow boiling in a straight mini tube

As a simple application of the peculiar solutions, the authors attempted flow boiling experiments in a single straight tube made of quartz and applied a high-carbon alcohol aqueous solution as the working fluid (Ono et al., 2008a). Figure 8(a) shows the flow loop used

in the experimental examination of convective boiling in the mini tube. A diaphragm pump was used to supply the fluid at a mass flux of 1–2 kg/m²s. A pressure tank was properly installed to eliminate the pressure beat caused by the pump. Figure 8(b) shows the test section in the experiment. A quartz glass tube was used as the test section. The tube was 1.0 mm in ID and 2.0 mm in OD. To provide Joule heating, a mixture of indium tin oxide (ITO) and silver was evenly sputtered on the outer surface of the tube. The film thickness was approximately 100 nm. Because the film is transparent, liquid motion inside the tube can be observed. Nine K-type thermocouples of 25 μm in OD were attached to the outer surface of the quartz tube with heat-resistant cement. The thermocouples were calibrated before performing the experiment by using a standard thermometer; their accuracy was confirmed to be within ±0.2 K. Simultaneously with temperature measurements, liquid motion was observed and recorded by a CCD video camera system. In mini tubes, the liquid temperature in flow boiling is strongly time dependent, as noted by other researchers (Thome, 2006; Cheng & Wu, 2006; Kandlikar, 2004). Also, in the present experiment, the temperature at the outer surface of the mini tube varied in a time dependent manner. The actual temperature data were very complicated; to investigate them quantitatively, they were time-averaged for analysis later. In this study, the flow rate was very small and was chosen so that dry-out phenomena could occur near the midpoint of the length of the tube. Moreover, the small flow rate made it easier to observe the liquid behaviour and liquid vaporisation. Temperature data were collected for approximately 60 min to obtain time-averaged values. Test fluids were 1-butanol aqueous solution (7.15 wt%), ethanol aqueous solution (7.15 wt%) and pure water. The solubility of 1-butanol in water at room temperature is 7.15wt%. The same concentration was adopted for the ethanol aqueous solution for comparison although the solubility of ethanol in water is much higher. Experimental conditions are shown in Table 1. Different quartz tubes and thermocouples were used in runs A and B.

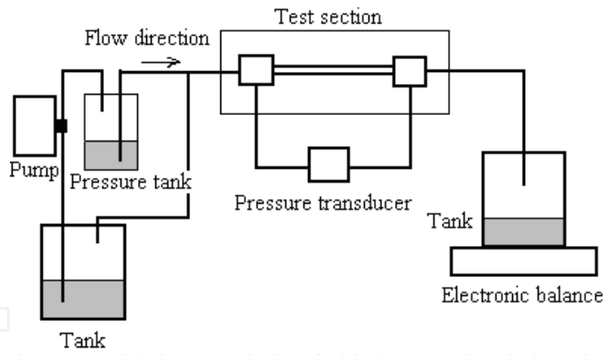

Fig. 8a. Experimental apparatus for the D_{in} = 1 mm channel.

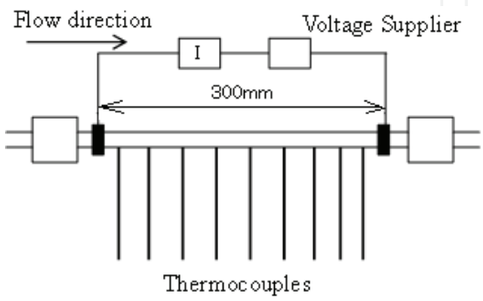

Fig. 8b. Test section of D_{in} = 1 mm.

Inner diameter D_{in} (mm)	Mass flow rate (kg/s)	Mass flux (kg/m²s)	Imposed heat flux (W/m²)	Re
1.0	1.7×10^{-6}	2.2	3.4×10^{6}	2.1

Table 1. Experimental conditions.

Figures 9(a1), (a2), (b) and (c) show images of the liquid behaviour near the dry-out position. Figures 10(a1), (a2), (b) and (c) show images from other experimental runs. In Figs. 9(a2) and 10(a2), curves are drawn to indicate the liquid–vapour interface because the position of the interface was somewhat difficult to see owing to the image quality. The dry-out position was approximately 240 mm away from the inlet, as estimated by a simple heat balance estimation. The dry-out phenomenon was in fact observed near this position. Figures 9(b) and 10(b) show results for pure water, and Figs. 9(c) and 10(c) show those for the ethanol aqueous solution. Figures 9(a1), 9(a2), 10(a1) and 10(a2) show that the butanol aqueous solution exhibited very peculiar liquid behaviour. The liquid film was elongated in the outlet direction, squeezed and separated into several smaller drops, and then it disappeared by vaporisation. This pattern of phenomena was sometimes repeated. In contrast, pure water and the ethanol aqueous solution did not exhibit such movement; they simply formed a relatively larger drop and disappeared by vaporisation.

Fig. 9.1a. Liquid behaviour of the butanol aqueous solution (7.15 wt%) (Run 1a).

Fig. 9.2a. Liquid behaviour of the butanol aqueous solution (7.15 wt%) (Run 1a).

Fig. 9b. Liquid behaviour of pure water (Run 1b).

Fig. 9c. Liquid behaviour of the ethanol aqueous solution (7.15 wt%) (Run 1c).

Fig. 10.1a. Liquid behaviour of the butanol aqueous solution (7.15 wt%) (Run 2a).

Fig. 10.2a. Liquid behaviour of the butanol aqueous solution (7.15 wt%) (Run 2a).

Fig. 10b. Liquid behaviour of pure water (Run 2b).

Fig. 10c. Liquid behaviour of the ethanol aqueous solution (7.15 wt%) (Run 2c).

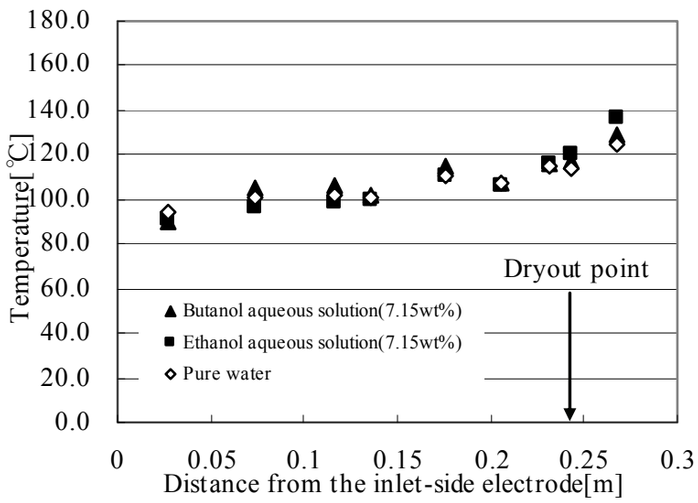

Fig. 11. Time-averaged temperature distribution at the tube surface (D_{in} = 1 mm).

The distribution of the time-averaged temperature at the outer surface of the tube is shown in Fig. 11. The position of the dry-out point, indicated in the figure, was estimated by a simple heat balance calculation ignoring surface tension phenomena. Observation results indicated that the estimated position was reasonable. On the basis of Fig. 11, the authors thought that under these experimental conditions, the butanol aqueous solution exhibited no apparent difference from pure water and the ethanol solution in terms of heat transfer. The butanol solution did exhibit peculiar movement of the evaporating liquid layer but the time-averaged dry-out position was not delayed. One reason for this could be the time span between the film elongation, shown in Fig. 9(a1), and the dry-out phenomenon for the butanol solution. The butanol solution exhibited a longer time span than pure water and the ethanol solution, and consequently, a larger temperature fluctuation. Therefore, even if the film elongation delayed the dry out, the longer dry-out

time span cancelled any advantage. Another reason could be the system design. In this simple straight tube, the temperature gradient in the longitudinal direction can not be increased much. The thermocapillary effect is generally enhanced by a larger temperature gradient. Thus, heating area should be localized, i.e. it should cover only a small area of the tube.

Next, the authors attempted an experiment in which the heated area was limited to only 10 mm in the longitudinal direction. It was assumed that the liquid would experience a higher temperature gradient at the region where the flow enters the small heated area. Figure 12 shows the test section used for this experiment. The length of the heated area differs from that in Fig. 8(b). The tube was the same quartz tube coated with the same mixture of ITO and silver; its ID was 1 mm and OD was 2 mm. An electrodes was set at each end of the heated length. As in the experiment in Fig. 8(b), nine thermocouples were glued to the outer surface of the tube. Table 2 lists experimental conditions and Table 3 lists specifications of test fluids.

The temperature of the outer surface at the midpoint of the heated region was measured to determine the cooling ability of the working fluid when a constant power of 3.5 W was applied to the heated area. The temperature was averaged from data taken over 30 min and is plotted in Figs. 13(a) and 13(b). Figure 13(b) shows an enlarged plot of the heated area. The temperature of the heated area was very high because the area became almost perfectly dry in the process. As shown in Fig. 13(b), the temperature of the butanol and pentanol aqueous solutions, which are nonlinear solutions, was approximately 70° lower than that of pure water. The temperature of the ethanol solution was also lower than that of pure water but the temperature difference was approximately 35°, and the cooling effect was weaker than that for butanol and pentanol solutions. The hexanol aqueous solution showed a weaker cooling effect than the ethanol solution although the hexanol solution is categorized as nonlinear. This contradiction requires further investigation. The authors think that it could be related to the high viscosity of the hexanol solution.

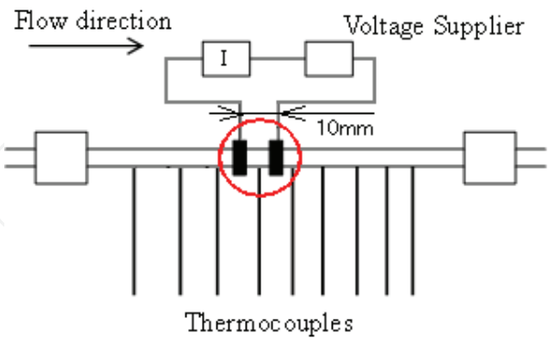

Fig. 12. Test section with the short heating length of D_{in} = 1 mm.

Inner diameter D_{in} (mm)	Mass flow rate (kg/s)	Mass flux (kg/m²s)	Imposed heat flux (W/m²)	Re
1.0	2.8×10^{-6}	3.6	1.1×10^{5}	12

Table 2. Experimental conditions (short heating length experiment).

Fluid	Concentration (wt%)
Butanol aq. sol.	7.15
Pentanol aq. sol.	2.0
Hexanol aq. sol.	0.58
Pure water	-
Ethanol aq. sol.	55

Table 3. Test fluids (short heating length experiment).

When the heating length was as large as 300 mm, as shown in Fig. 8(b), the solution switched to the vapour phase in a complicated manner through the entire length of the heated region. However, in the experiment with the very short heated region shown in Fig. 12, the solution quickly changed to a liquid layer and then to vapour near the entrance to the heated region. This made the observation rather simple and the dry out was readily detected.

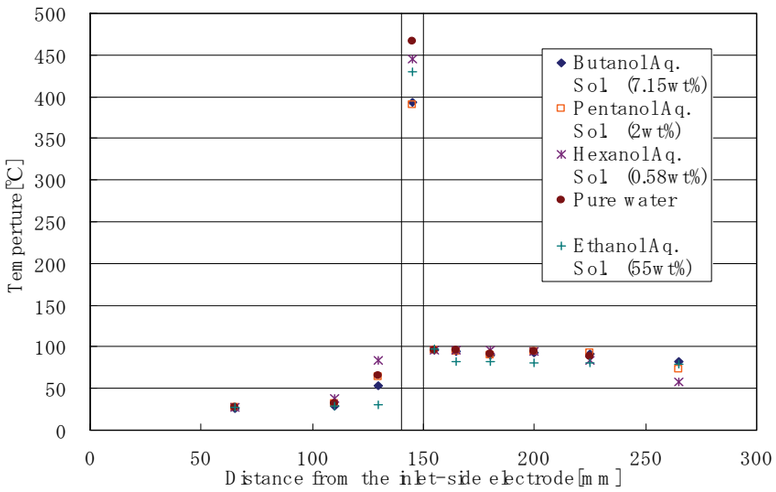

Fig. 13a. Distribution of temperature at the outer surface of the tube.

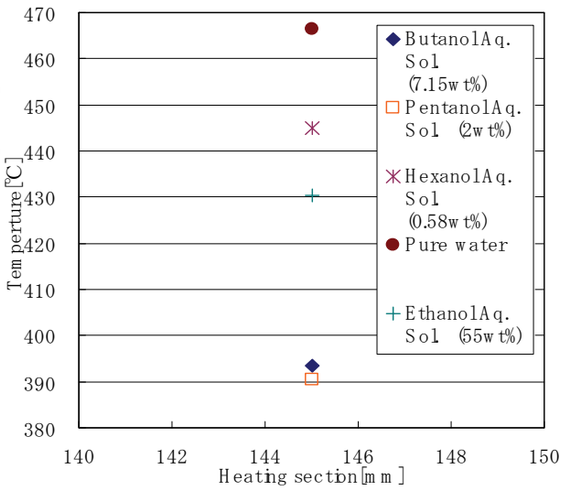

Fig. 13b. Distribution of temperature at the outer surface of the heated section.

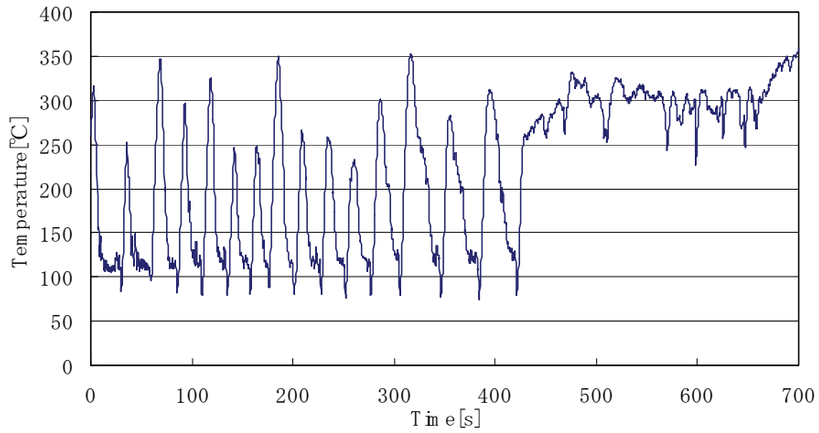

Fig. 14. Temperature fluctuation at the outer surface (butanol aqueous solution).

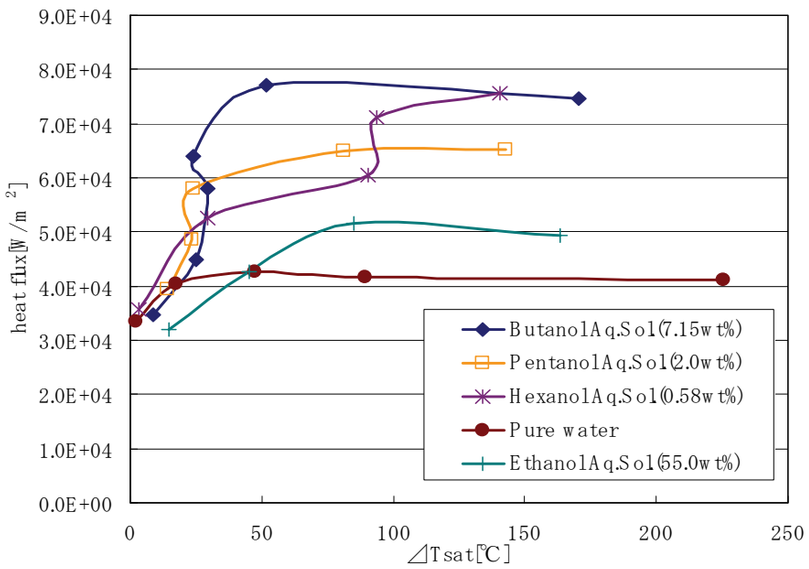

Fig. 15. Boiling curves of all test fluids.

The authors investigated the onset of the dry out state by gradually increasing the applied power. Figure 14 shows the temperature fluctuation before and after the onset of the dry out for the butanol aqueous solution. Before the perfect dry out occurred, the temperature fluctuated strongly. When the liquid layer evaporated, the temperature rapidly increased; however, once the liquid further entered the heated region, the temperature quickly decreased to a value approximately equal to the saturated temperature. However, when the power increased, the liquid could no longer remain in the heated area and it evaporated as soon as it entered the region. At this point, the temperature became extremely high, and the inner surface of the tube became perfectly dry.

This dry-out pattern was very unusual because the flow rate was quite small and the temperature of the dried wall was extremely high in this study. Thus, the detected dry-out heat flux might not be readily comparable to the heat flux of conventional dry-out phenomena, which should be noted when referring to other researchers' data.

The authors investigated the heat flux at the unusual dry-out point described above by changing the type of fluid. Figure 15 shows boiling curves obtained in those experiments. The heat flux was corrected by reducing the heat loss to environmental air and to the surrounding quartz region by heat conduction. The heat loss was estimated by performing a preliminary experiment without flowing liquid whose details are omitted here. Note that the heat flux was very small because the flow rate was quite small in these experiments. As shown in Fig. 15, maximum heat fluxes obtainable with nonlinear solutions, namely the butanol and pentanol aqueous solutions, were larger than those of other fluids. The authors considered that those nonlinear solutions tended to wet the heated surface more than other fluids owing to their peculiar characteristics, and that the dry-out state was delayed as a result. This difference was made clear by adopting a short heating region. The large temperature gradient that was realized near the entrance of the heated area could have intensified the nonlinear thermocapillary effect.

In summary, the authors attempted a very special type of a situation for applying a very large temperature gradient to a liquid layer of a nonlinear solution and succeeded in obtaining more desirable characteristics of the solution. However, under this condition, the heat flux at the dry-out point was too small for application in practical methods. Therefore, further ideas and modifications, including changes to the flow pattern and heating system, are needed to obtain a practical level of the heat flux. The authors began modifying the experimental setup after experiments shown in Section 3.

4. Modified application to flow boiling in T-junction mini tube

In the previous section, the butanol aqueous solution was found to exhibit better heat transfer characteristics as long as it experienced a large temperature gradient over a short heating region. However, in previous experiments, the obtained heat flux was very small and was not in the range of practical application. As a more practical experiment, the authors set up new test sections of T-junction mini channels. In this flow pattern, the fluid could impinge on the heated surface and flow away with boiling bubbles to the outlet. Therefore, the temperature boundary layer can be thinned, and also, as shown in Fig. 16, the temperature gradient around the boiling bubble located on the heated surface can be increased. The thermocapillary effect is expected to work more strongly under this temperature gradient.

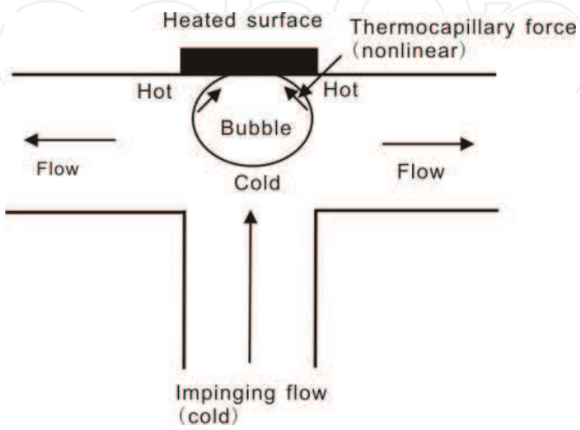

Fig. 16. Impinging flow pattern with boiling when using a nonlinear solution.

Here the authors attempted two types of test sections. One is a T-junction mini tube made of transparent quartz for observation, and the other is a T-junction made of insulating polymer material for localizing heat transfer at the heated surface to obtain precise heat flux values.

4.1 T-junction mini tube made of quartz glass

A schematic of the flow system is shown in Fig. 17. The T-junction channel was made of quartz glass. The heated surface was the edge of a copper block that contained a rod heater inside. DC power was applied to the rod heater. Figure 18 shows details of the T-junction test section. The inside cross-sectional area of the channel was 2 mm × 2 mm and outer dimensions of the cross section were 4 mm × 4 mm. The entire length was 150 mm. At the middle of the upper surface of the horizontal channel, a slit of a cross-sectional area of 2 mm × 10 mm was prepared for inserting the edge of the copper block. A vertical channel of 75 mm was added to form a T-junction channel. The geometry of the copper block is shown in Fig. 19. The fluid contacted the left edge. The surface was polished by using #3000 emery paper. Three K-type thermocouples were inserted near the edge of the copper block. The thermocouples were located 3 mm, 7 mm and 11 mm from the contacting surface, respectively. The temperature gradient and heat flux were deduced from the obtained temperature data by applying the simple one-dimensional Fourier law. The surface temperature at the edge was also calculated by extrapolation from the data. The motion of the liquid and boiling bubbles was observed by using a video camera. Experimental conditions are shown in Table 4. Test fluids were butanol aqueous solutions of 3.00 wt% and 7.15 wt% and pure water.

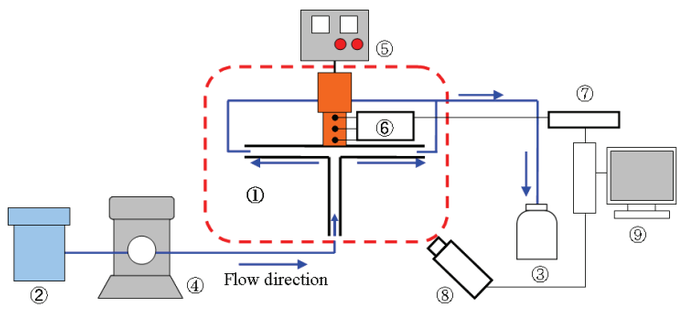

1: Test section; 2, 3: Tank; 4: Metering pump; 5: DC power supply; 6: Thermocouples; 7: Thermocouple logger; 8: Video camera and 9: PC

Fig. 17. Experimental apparatus (T-junction mini tube made of quartz glass).

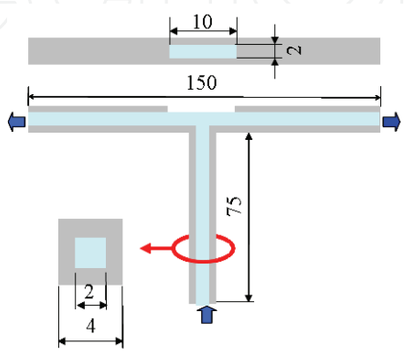

Fig. 18. Test section (T-junction mini tube made of quartz glass).

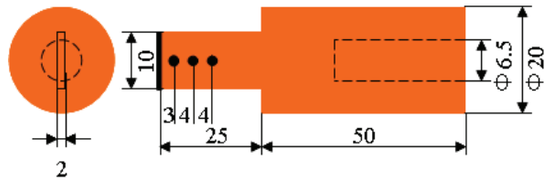

Fig. 19. Copper block used for heating.

Mass flow rate (kg/s)	Mass flux (kg/m²s)	Re	Subcooling (K)
1.4×10^{-4}	35	79	75

Table 4. Experimental conditions (T-junction mini tube made of quartz glass).

Figures 20(a), 20(b) and 20(c) show images of observations of the nucleate boiling state. The images are not of high quality; therefore, large boiling bubbles are outlined in white. The observed area included the heated surface and its periphery.

When butanol solutions were used, two types of boiling bubble were observed. One was fine bubbles that cannot be seen in Figs. 20(a) and 20(b). The fine bubbles quickly detached from the heated surface and moved away. The 3.00 wt% butanol solution produced more bubbles of this type than the 7.15 wt% solution. The other type was relatively large bubbles located on the heated surface, which are outlined in Fig. 20. They remained at the surface for some time and then became detached. This type of bubble was smaller in the 7.15 wt% solution than in the 3.00 wt% solution. In pure water, only large bubbles were observed and no fine bubbles were detected.

Near the CHF (abbreviation of Critical Heat Flux) or the dry-out condition, the large bubbles coalesced and formed an extended bubble that occasionally covered the heated surface. However, when butanol solutions were used, the liquid layer seemingly covered the heated surface again inside the bubble when such an extended large bubble appeared on the heated surface. Numerous fine boiling bubbles were detected on the heated surface through the extended bubble covering the heated area.

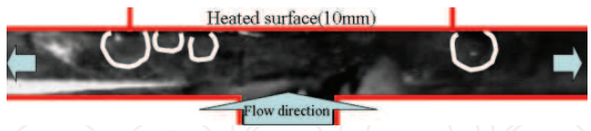

(a) Butanol aq.sol (3.00wt%)

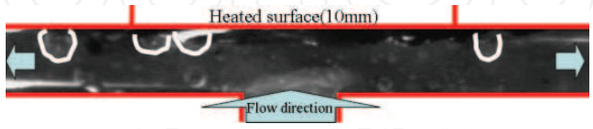

(b) Butanol aq.sol (7.15wt%)

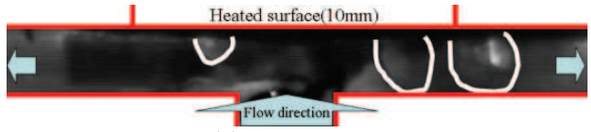

(c) Pure water

Fig. 20. Images of observed motion (T-junction mini tube made of quartz glass).

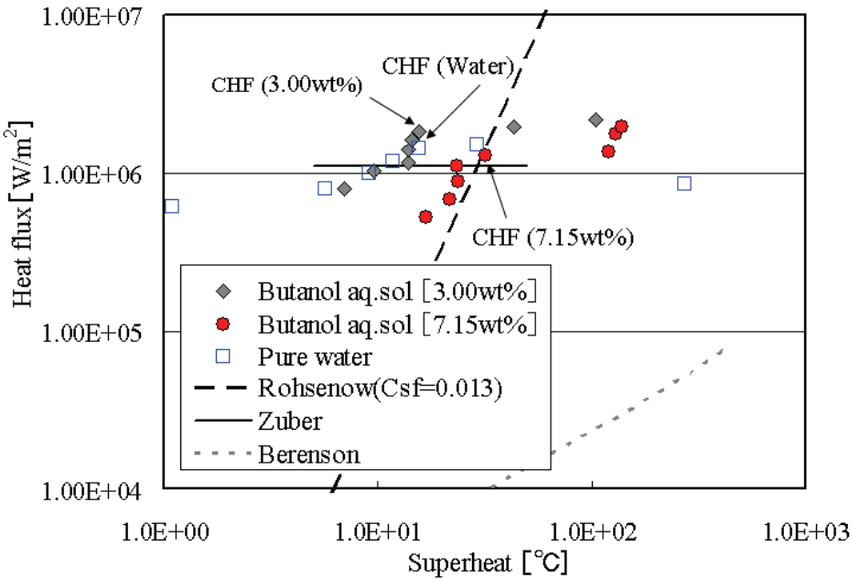

Fig. 21. Boiling curves (T-junction mini tube made of quartz glass).

Boiling curves are shown in Fig. 21. Several well-known correlation lines are also shown for reference: Rohsenow's nucleate boiling relationship (Rohsenow, 1952), Zuber's prediction of CHF (Zuber, 1958) and Berenson's film boiling relationship (Berenson, 1961). All of them are detailed in standard textbooks (e.g. Carey, 1992) and their explanations are omitted here. Rohsenow's equation will be mentioned briefly in the next section.

CHF points or dry-out points are indicated for each fluid in Fig. 21. These points were determined by finding the beginning of the decrease in the heat transfer coefficient when viewed as a function of heat flux. After CHF points, the so-called post dry-out state was detected. The CHF flux of the 7.15 wt% butanol solution was slightly lower than that of pure water. This can be explained by the mechanism of the so-called degradation of the boiling heat transfer of binary mixtures. A concentration of 7.15 wt% was considered large, and the change in the saturated temperature, owing to alcohol evaporation, was large. On the other hand, the CHF value of the 3.00 wt% butanol solution was approximately 30% higher than that of pure water. The 3.00 wt% solution exhibited an interesting characteristic near the CHF. Before reaching the CHF, heat transfer was remarkably enhanced, and the heat transfer coefficient increased considerably, as shown in Fig. 21.

This characteristic is believed to be related to peculiar bubble behaviour near the dry-out state, which requires further investigation. Note that the degradation of boiling heat transfer did not occur strongly in the 3.00 wt% and 7.15 wt% butanol aqueous solutions. CHF values of those solutions were approximately equal to those of pure water. However, that of the 3.00 wt% butanol solution was increased to some extent. The authors speculate that the reason is that the combined thermocapillary and solutocapillary effects were active at bubble surfaces.

4.2 T-junction mini tube made of polymer material

As mentioned in the previous section, the glass tube was useful for observing the overall behaviour of boiling bubbles on the heated surface and detached and flowing bubbles in the channel. However, in practical applications, fragile glass would be difficult to employ in real

systems. In most cases, a polymer material or metal would be used for small packaged systems. Here, to simplify the heat transfer analysis, an insulating polymer material was selected. Specifically, in studying the contribution of convective heat transfer, the insulating wall can become a simple boundary condition. Figure 22 shows the test section made of polyether ether ketone (PEEK) material, which has good heat resistance. A channel of a cross-sectional area of 3 mm × 3 mm was made in the polymer plate. The channel was 100 mm long, and from its midpoint, a vertical channel that was 50 mm long was added for the inlet flow. At the region in contact with the vertical inflow, a copper surface was installed. The copper surface was the edge of a copper block having a similar structure to that described in the previous section. Inside the copper block, a heater rod was inserted, and DC power was applied to provide Joule heating. Near the edge, three thermocouples were inserted to obtain the surface temperature, the temperature gradient and the heat flux, as in the previous section. The heated surface that contacted the fluid was 3 mm × 10 mm in area. Although bubble observation was not as simple as in the glass channel experiment, it was enabled by incorporating a glass window near the heated surface, as shown in Fig. 22. A video camera recorded images and transmitted data to a PC. At the inlet and outlet positions of the test section, thermocouples were also installed to monitor the temperature. Experimental conditions are shown in Table 5. Test fluids here were the 7.15 wt% butanol aqueous solution and pure water.

Snapshots edited from the recorded video images are shown in Fig. 23. When pure water was used, the heated surface was occasionally covered with a vapour blanket, as shown in Fig. 23(b), and bubbles had a flattened shape. On the other hand, when the 7.15 wt% butanol aqueous solution was used, boiling bubbles became much smaller and detached from the heated surface smoothly, as shown in Fig. 23(a). The shape of bubbles in the butanol solution was rather spherical and they moved smoothly on the heated surface before detaching. The difference in shape was attributed partly to the difference in the contact angle between the copper surface and the fluid. The contact angle between pure water and the copper surface was 94°, and that between the 7.15 wt% butanol aqueous solution and the copper surface was 51°, according to the authors' measurements at 25 °C. Regarding the bubble detachment and their movement in the butanol solution, the authors think that the small contact angle and the Marangoni effect worked simultaneously.

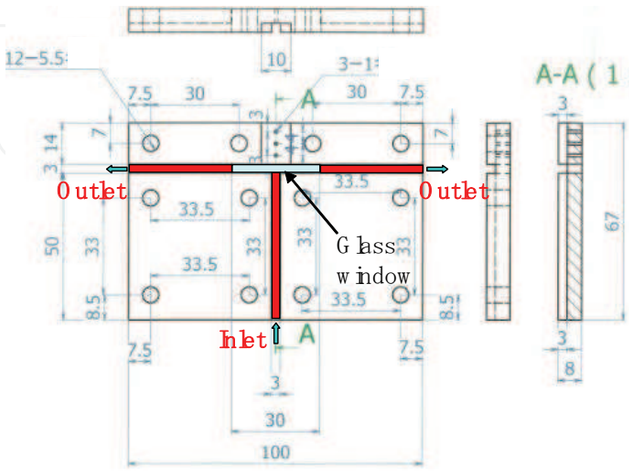

Fig. 22. Test section (T-junction mini tube made of polymer material).

Mass flow rate (kg/s)	Mass flux (kg/m²s)	Re	Subcooling (K)
6.7×10^{-5}	7.4	78	20

Table 5. Experimental conditions (T-junction mini tube made of polymer material).

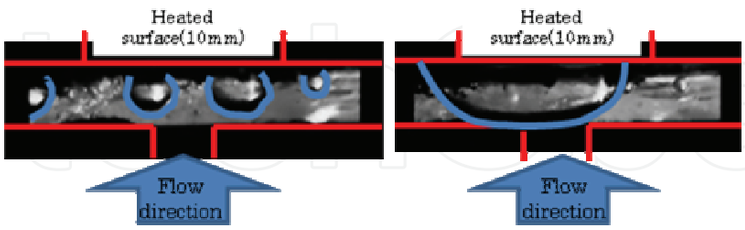

(a)Butanol aq.sol.(7.15wt%) (b)Pure water

Fig. 23. Behaviour of boiling bubbles (T-junction mini tube made of polymer material).

Figure 24 shows boiling curves; Rohsenow's correlation line is shown for reference. Curve obtained by Katto's equation for single-phase convective heat transfer in two-dimensional flow impingement (Katto, 1981) and that obtained by Hausen's equation for single-phase convective heat transfer in a simple tube (Hausen, 1943) are also shown.
Note that owing to technical difficulties with the experimental apparatus, these experiments did not reach the dry-out condition. When the T-junction channel was used, the heat flux of the butanol solution was approximately 1.2 times larger than that of pure water. This difference was thought to be caused by the difference in bubble movement. The increase in the heat flux when the butanol solution was used was not as dramatic in the experiment but the degradation of the boiling heat transfer of binary mixtures was not observed, as in the case of the T-junction mini tube made of quartz glass.

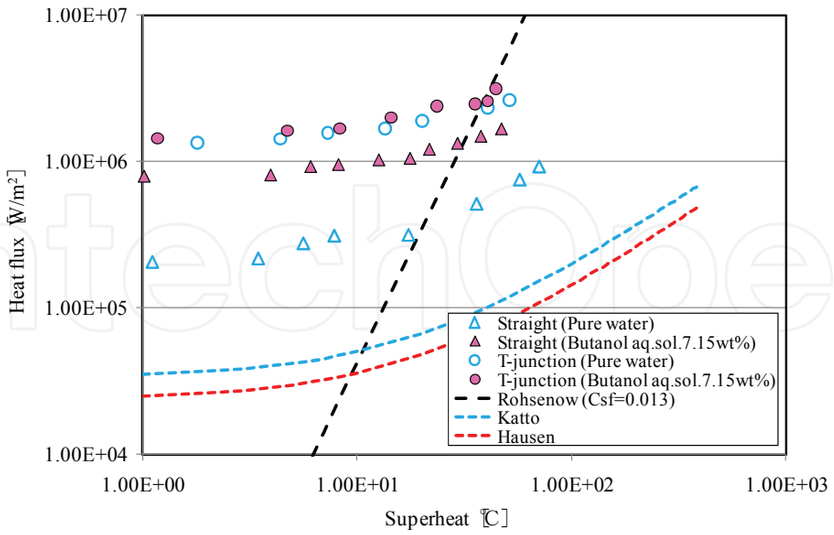

Fig. 24. Boiling curves (T-junction and straight mini tube made of polymer material).

As a comparison, the authors performed the same experiments with a straight channel. These results are also shown in Fig. 24. It can be readily understood from the effect of the impinging flow pattern that the heat flux in the straight channel was much lower than that

in the T-junction channel. Also, in the straight flow pattern, the heat flux in the butanol solution was larger than that in pure water. Moreover, it is very interesting that the degree of enhancement when the butanol solution was used was much greater in the straight channel than in the T-junction channel. This suggests that the Marangoni effect influenced boiling bubbles.

For comparison with well-known correlations, the authors plotted Rohsenow's equation for nucleate pool boiling, Katto's equation for heat transfer with a single-phase impinging flow and Hausen's equation for convective heat transfer with a single-phase channel flow.

The authors adopted Rohsenow's equation because the flow rate was very small in this experiment, and thus, once strong nucleate boiling occurred, the boiling could be regarded as nearly the same as pool boiling. Rohsenow's equation is as follows.

$$h = \left[\frac{k_l \mathrm{Pr}_l^{-0.7}}{l_a C_{sf}} \left(\frac{\Delta T_{sat} l_a}{\rho_l \nu_l L_{lv}} \right)^{0.67} \right]^{1/0.33} \tag{3}$$

$$l_a = \sqrt{\frac{\sigma}{g(\rho_l - \rho_v)}} \tag{4}$$

Here, h is the heat transfer coefficient, l_a is the Laplace length, k_l is the thermal conductivity of the fluid and ν_l is its dynamic viscosity. L_{lv} is the latent heat. Pr_l is the Prandtl number of the fluid, g is the gravitational acceleration, ρ_l is the density of the liquid and ρ_v is that of the vapour. ΔT_{sat} is the super heat of the wall. C_{sf} is an empirical parameter describing the combination of wall material and fluid. Here, the surface tension of the fluid, σ is the value of pure water at the saturated temperature and its temperature dependence is not included so that we can represent properties of butanol solutions. A method of incorporating the peculiar surface tension of butanol solutions remains to be studied in the future. The resulting heat flux can be expressed as follows.

$$q = h(T_w - T_s) \tag{5}$$

Here, q is the heat flux and h is the heat transfer coefficient. T_w and T_s are the wall temperature and the saturated temperature, respectively. Katto's equation is as follows.

$$q = 0.570 \mathrm{Pr}_l^{0.4} \frac{k_l}{x} \sqrt{\frac{u_\infty x}{\nu_l}} (T_w - T_l) \tag{6}$$

This equation applies only to two-dimensional flows. For reference, the deduced heat flux was adopted only for comparison with the experimental data. T_l is the temperature of the flow at the inlet, u_∞ is the representative velocity of the flow and x is the distance from the centre of the flow impingement. Hausen's equation is as follows.

$$q = \left\{ 3.66 + \frac{0.0668 G_{zL}}{1 + 0.04 G_{zL}^{2/3}} \right\} \frac{k_l}{D} (T_w - T_l) \tag{7}$$

Originally, this equation is applied to round tubes. For application to the experiment in this study, the deduced heat flux was adopted for comparison with the experimental data. D is

the effective diameter of the channel. G_{zL} is the Graetz number, which can be defined as follows.

$$G_{zL} = \mathrm{Re}_D \mathrm{Pr}_l \frac{D}{L} \tag{8}$$

L is the length of the heated region. Re_D is the Reynolds number, which is defined as follows.

$$\mathrm{Re}_D = \frac{uD}{\nu_l} \tag{9}$$

Here, u is the averaged velocity in the channel. As shown in Fig. 24, the measured heat flux data were larger than values obtained by Katto's and Hausen's equations. This is because experiments included boiling heat transfer as well as convective heat transfer. However, not all the data seemed to obey Rohsenow's curve although the observation apparently revealed that weak nucleate boiling occurred. The authors think that the boiling in experiments was so weak that the heat transfer caused by boiling did not contribute much to the entire heat flux. New experiments in which the applied power can be increased to obtain both a strong nucleate boiling and a dry out will be needed for further investigation. The authors are now preparing such experiments to investigate the onset of the dry out and will report them in the near future.

When the glass channel described in the previous section was used, the heat transfer improved abruptly near the dry-out point, as shown in Fig. 21. The authors expect that similar phenomena could occur in the polymer channel. Moreover, polymer material is generally hydrophobic; therefore, bubbles are less likely to stick to the surface. Thus, once boiling bubbles detach from the copper surface, they leave the copper surface smoothly and maintain heat transfer caused by their motion. These issues must be examined in future experiments.

Although the above limitation existed in the current data, the authors believe that advantages of the butanol aqueous solution were clarified to some extent. In a prototype system made of insulating polymer material, the butanol aqueous solution can be thought to have the potential to enhance heat transfer in boiling with flow impingement inside mini channels.

5. Conclusion

The authors have been performing various types of experiment to clarify and demonstrate advantages of high-carbon alcohol aqueous solutions for boiling heat transfer inside mini channels after confirming peculiar characteristics of the temperature dependence of surface tension by their own measurements. Findings and conclusions to date can be summarized as follows.

1. To investigate the peculiar temperature dependence of the surface tension of butanol and other high-carbon alcohol aqueous solutions, a static maximum bubble pressure method was adopted, and measurements were performed. These measurements revealed the nonlinearity of the surface tension of those solutions and provided more reliable data than those obtained by Wilhelmy's method.
2. When a butanol solution was applied to a simple long mini tube of 1 mm in diameter, the dry out was not delayed by using the solution. However, very unusual behaviour of

the liquid layer, namely an extending motion of the liquid layer to a hotter region, was observed.

3. When the heating region was localized in the mini tube to obtain a large temperature gradient at the entrance of the region, the dry-out heat flux under a very small flow rate was larger when the high-carbon alcohol aqueous solution was used. However, owing to technical difficulties, this experiment had a heat flux of a very small order.
4. A T-junction mini channel was studied because this flow pattern could increase the temperature gradient around boiling bubbles remaining on the heated surface. Experiments revealed that the use of butanol aqueous solutions increased the dry-out heat flux somewhat in a T-junction channel made of glass. When a T-junction channel made of polymer material was used, the heat flux before the onset of the dry out was again somewhat increased by using these solutions.

As aforementioned, the authors are certain that high-carbon alcohol aqueous solutions can induce peculiar motion in the liquid layer and boiling bubbles. However, the advantage in heat transfer was not as dramatic and was limited to small values. On the other hand, some examples of their good characteristics were reported in pool boiling and large heat pipes (Abe, 2006a, 2006b). More modifications of flow conditions and flow patterns would be needed for adaption to the small-scale environment of mini channels.

Another important issue requiring investigation is the mechanism of the Marangoni force acting on boiling bubbles. As long as an alcohol aqueous solution is used, the thermocapillary and solutocapillary forces will always coexist. In particular, when a butanol solution is used, directions of the two forces are the same; therefore, it is not yet clear which of the two forces is dominant in boiling bubbles. The authors began to observe the onset of the Marangoni convection around a small air bubble in a butanol aqueous solution (Eda et al., 2010). These results indicated a clear contribution of a peculiar thermocapillary force. They now plan to clarify the contribution ratio of each capillary force in butanol aqueous solutions.

6. Acknowledgements

The authors would like to thank Prof M. Shoji, Mr S. Nishiguchi, Dr T.-H. Yen, Dr F. Takemura, Dr S. Matsumoto and Dr M. Tange for their helpful suggestions and aid in the research. They are also grateful to Mr T. Yoshida, Mr T. Kaneko, Mr M. Otsuka, Mr Y. Kumagai, Mr K. Kunimatsu, Mr K. Kawai, Mr T. Ueno and Mr Y. Nomura for their assistance in the experiments and measurements. This research was partially supported by the MEXT/JSPS, Grant-in-Aid for Scientific Research (C, No. 21560225).

7. References

Abe, Y. (2006a). Thermal management with self-rewetting fluids, *J. Jpn. Soc. Microgravity Appl.,* Vol. 23, No. 2 (2006), pp. 80–87.

Abe, Y. (2006b). Self-rewetting fluids, *Ann. N.Y. Acad. Sci.* 1077 (2006), pp. 650–667.

Adamson, A.W. & Gast, A.P. (1997). Physical chemistry of surfaces, A Wiley-Interscience publication (1997).

Azouni, M.A. & Petre, G. (1998). *J.Colloidal Int. Sci.*, 206 (1998), pp. 332–333.

Berenson, P. J. (1961). Film boiling heat transfer from a horizontal surface, *J. Heat Transfer*, Vol. 83, pp. 351, 1961.

Carey, V. P. (1992). Liquid-Vapor Phase-Change Phenomena, (1992), Taylor and Francis.

Cheng, P. & Wu, H.Y. (2006). Phase-change heat transfer in Microsystems, 13th International Heat Transfer Conference, Key Note-02, 13–18 August, Sydney, Australia.

Eda, Y., Kawai, K. & Ono, N. (2010). Observation of marangoni flow near the artificial air bubble on heated surface in using alcohol aqueous solution, Seventh International Conference on Flow Dynamics (1–3 November 2010, Sendai, Japan), Proceedings pp. 448–449.

Hausen, H. (1943). VDI Z., No. 4, pp. 91, 1943, In: Heat transfer, Hallman, J.P., McGraw-Hill, 1976.

JSME Data Book: Thermophysical Properties of Fluids (1983), JSME (in Japanese).

Kandlikar, S.G. (2004). Heat transfer mechanisms during flow boiling in microchannels, *J. Heat Transfer (Transactions ASME)*, 126 (2004), pp. 8–16.

Katto, Y. (1981). In: JSME Data Book: Heat Transfer, 5th Edition (2009), JSME (in Japanese), pp. 33.

Legros, J.C. (1986). *Acta Astronautica*, 13–11 December 1986, pp. 697–703.

Ono, N., Yoshida, T., Kaneko, T., Nishiguchi, S. & Shoji, M. (2009). *Journal of Thermal Science and Technology* (JSME), Vol.4 (2009), No.2, pp.284-293.

Ono, N., Yoshida, T., Kaneko, T., Nishiguchi, S. & Shoji, M. (2008a). *Thermal Science and Engineering*, Vol. 16, No.3 (2008), pp. 79–85.

Ono, N., Kaneko, T., Nishiguchi, S. & Shoji, M. (2008b). *Proceedings of IFHT2008*, (2008), Paper No. 200, CD-ROM.

Rohsenow, W.M. (1952). A method of correlating heat transfer data for surface boiling liquids, *Trans. ASME*, Vol. 74, pp.969, 1952.

Thome, J.R. (2006). Fundamentals of boiling and two-phase flows in microchannels, 13th Inter-national Heat Transfer Conference, Key Note-14, 13–18 August, Sydney, Australia.

Vochten, R. & Petre, G. (1973). Study of the heat of reversible adsorption at the air-solution interface, *J.Colloidal Science*, 42-2(1973), pp. 320–327.

Zuber, N. (1958). On the stability of boiling heat transfer, *Trans. ASME*, Vol. 80, pp.711, 1958.

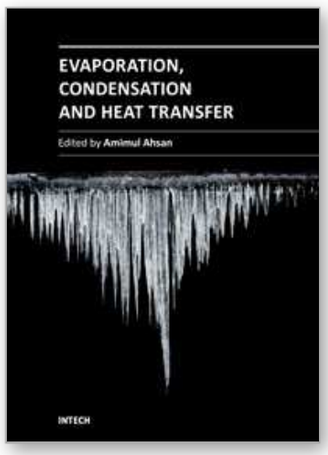

Evaporation, Condensation and Heat transfer
Edited by Dr. Amimul Ahsan

ISBN 978-953-307-583-9
Hard cover, 582 pages
Publisher InTech
Published online 12, September, 2011
Published in print edition September, 2011

The theoretical analysis and modeling of heat and mass transfer rates produced in evaporation and condensation processes are significant issues in a design of wide range of industrial processes and devices. This book includes 25 advanced and revised contributions, and it covers mainly (1) evaporation and boiling, (2) condensation and cooling, (3) heat transfer and exchanger, and (4) fluid and flow. The readers of this book will appreciate the current issues of modeling on evaporation, water vapor condensation, heat transfer and exchanger, and on fluid flow in different aspects. The approaches would be applicable in various industrial purposes as well. The advanced idea and information described here will be fruitful for the readers to find a sustainable solution in an industrialized society.

InTech Europe
University Campus STeP Ri
Slavka Krautzeka 83/A
51000 Rijeka, Croatia
Phone: +385 (51) 770 447
Fax: +385 (51) 686 166
www.intechopen.com

InTech China
Unit 405, Office Block, Hotel Equatorial Shanghai
No.65, Yan An Road (West), Shanghai, 200040, China
中国上海市延安西路65号上海国际贵都大饭店办公楼405单元
Phone: +86-21-62489820
Fax: +86-21-62489821

IntechOpen